HHS Public Access

Author manuscript

Bioelectrochemistry. Author manuscript; available in PMC 2019 August 01.

Published in final edited form as:

Bioelectrochemistry. 2018 August ; 122: 123–133. doi:10.1016/j.bioelechem.2018.03.014.

The second phase of bipolar, nanosecond-range electric pulses determines the electroporation efficiency

Andrei G. Pakhomov[*,a], **Sergey Grigoryev**[a], **Iurii Semenov**[a], **Maura Casciola**[a], **Chunqi Jiang**[a,b], and **Shu Xiao**[a,b]

[a]Frank Reidy Research Center for Bioelectrics, Old Dominion University, Norfolk, VA 23508, USA

[b]Department of Electrical and Computer Engineering, Old Dominion University, Norfolk, VA 23508, USA

Abstract

Bipolar cancellation refers to a phenomenon when applying a second electric pulse reduces ("cancels") cell membrane damage by a preceding electric pulse of the opposite polarity. Bipolar cancellation is a reason why bipolar nanosecond electric pulses (nsEP) cause weaker electroporation than just a single unipolar phase of the same pulse. This study was undertaken to explore the dependence of bipolar cancellation on nsEP parameters, with emphasis on the amplitude ratio of two opposite polarity phases of a bipolar pulse. Individual cells (CHO, U937, or adult mouse ventricular cardiomyocytes (VCM)) were exposed to either uni- or bipolar trapezoidal nsEP, or to nanosecond electric field oscillations (NEFO). The membrane injury was evaluated by time-lapse confocal imaging of the uptake of propidium (Pr) or YO-PRO-1 (YP) dyes and by phosphatidylserine (PS) externalization. Within studied limits, bipolar cancellation showed little or no dependence on the electric field intensity, pulse repetition rate, chosen endpoint, or cell type. However, cancellation could increase for larger pulse numbers and/or for longer pulses. The sole most critical parameter which determines bipolar cancellation was the phase ratio: maximum cancellation was observed with the 2nd phase of about 50% of the first one, whereas a larger 2nd phase could add a damaging effect of its own. "Swapping" the two phases, i.e., delivering the smaller phase before the larger one, reduced or eliminated cancellation. These findings are discussed in the context of hypothetical mechanisms of bipolar cancellation and electroporation by nsEP.

[*]Corresponding author: Andrei G. Pakhomov, Frank Reidy Research Center for Bioelectrics Old Dominion University 4211 Monarch Way., Suite 300, Norfolk, VA 23508 +1(210)2049012, +1(757)6838003, Fax: +1(757)4511010, 2andrei@pakhomov.net; apakhomo@odu.edu.

Conflicts of interest

None.

Author contributions

A.G.P. conceived and designed the study; A.G.P., I.S., and S.G. conducted the experiments and analyzed the data; M.C. performed EF simulations for dosimetry calculations; S.X. and C.J. designed and fabricated the pulser; all authors discussed and interpreted the data; A.G.P. wrote the manuscript.

Keywords

Nanosecond pulses; Electroporation; Electropermeabilization; Nanopores; Membrane permeability; Bipolar cancellation

1. Introduction

It was shown for the first time in 2015 that bipolar nanosecond electric pulses (nsEP) are far less efficient at electroporating cell membrane than unipolar pulses of the same total duration and amplitude[1]. This observation was extended to bipolar pulses which were twice the duration of a unipolar pulse; in other words, adding the second, opposite polarity phase to a unipolar nsEP reduced it bioeffects, despite delivering twice more energy[2]. For example, the addition of the opposite polarity second phase reduced Ca^{2+} mobilization, YP uptake, and cell killing by nsEP [2–5]. Since a bipolar pulse is essentially a succession of two unipolar pulses of the opposite polarities, the reduction of its biological efficiency means that the delivery of the second pulse of the opposite polarity cancels the effect of the first pulse. This paradoxical response, named “bipolar cancellation,” is preserved when the two phases are separated in time into two unipolar nsEP of opposite polarities, and gradually tapers out as the interval between them increases. The bipolar cancellation could still be observed for pulse separations of up to 10 μs[2] or even 50 μs[3]. The reason for choosing the term “cancellation” rather than “inhibition” or “attenuation” was the fact that the first pulse ends long before the second pulse arrives to halt the chain of events triggered by the first pulse, thereby “canceling” already “scheduled” permeabilization. Bipolar stimulation is characteristic for nanosecond range of pulse durations (perhaps also including the lower microsecond range) and has not been observed for conventional multi-microsecond and millisecond pulse electroporation [6–13].

This reversibility of the initial steps of membrane electropermeabilization cannot be easily explained by the existing concepts of nsEP interaction with biomembranes[2]. An “assisted membrane discharge” hypothesis suggests the reversal of the external field facilitates the discharge of cell plasma membrane, thereby reducing electroporative damage. This hypothesis assumes that the supra-critical membrane potential is preserved across the membrane for long time after it was charged by the first pulse, so the pore formation continues during the discharge – unless the discharge is expedited by applying the electric field in the opposite direction. However, the time intervals which still enable the bipolar cancellation (up to 50 μs[3]) are far greater than the calculated cell discharge times of under 1 μs for intact membranes[14], and supposedly much faster discharge of already electroporated membranes. Increasing the conductance of the medium was expected to expedite the membrane discharge and thereby shorten the interpulse interval “window” for bipolar cancellation, but no such shortening was observed[3].

Another elegant idea, that the reversal of Ca^{2+} drift might be responsible for cancellation[15], was challenged by observations of bipolar cancellation in the absence of Ca^{2+} and by the fact that the increase of membrane electrical conductance by nsEP is also subject to cancellation[4]. Whereas possible contribution of the reversal of Ca^{2+} drift to

bipolar cancellation can still be considered, it has been ruled out as the only or the main mechanism of cancellation. A recently proposed “hybrid” hypothesis tried to combine the assisted membrane discharge and electrophoretic drift to explain peculiarities of YP dye uptake caused by bipolar pulses of various configuration[16]; however, the authors’ own data in the same paper, as well as other studies[3, 17–19], show that practically all YP uptake occurs during a long (seconds to minutes) time interval after nsEP and therefore is independent of drift.

Other suggested mechanisms awaiting experimental validation include a two-step chemical process, such as with ROS formation as the reversible first step and membrane oxidation as the next step, and the reduction of electrodeformation forces by pulse polarity change[2, 3]. The search for a membrane permeabilization mechanism which starts with a process reversible within microseconds after nsEP is presently going on; its importance is emphasized by the fact that such reversal is not predicted or understood within the existing electroporation paradigms, hence a substantial revision of these paradigms is likely once the mechanisms underlying the bipolar cancellation are identified.

Quantifying the bipolar cancellation within a multi-dimensional space of various electric pulse parameters (including pulse duration, shape, amplitude, number and repetition rate of pulses, the interval between opposite polarity pulses, etc.), in different types of cells and tissues, and using different endpoints defines boundaries for identifying the mechanism(s) responsible for cancellation. Recent studies confirmed bipolar cancellation for nanosecond electric pulse oscillations (NEFO)[4] and for asymmetrical bipolar nsEP, with the second phase made longer or shorter than the first one[16]. Here, we extended these studies by focusing primarily on the amplitude ratio of phases of a bipolar pulse. Concurrently, we tested the effects of the pulse number and repetition rate, and compared NEFO and traditional trapezoidal pulses. In additional to cell lines commonly used for such studies (such as CHO and U937), for the first time we explored bipolar cancellation in primary ventricular cardiomyocytes (VCM), which are profoundly different from the other cells in size, shape, and physiology. We confirmed bipolar cancellation as a common phenomenon, for all tested cell types and for most tested pulsing conditions. We demonstrated that, for diverse experimental conditions and endpoints, the maximum cancellation is reached when the amplitude of the second phase of a bipolar pulse is set at about 50% of the first phase. This dependence is reasonably explained by increasing membrane damage by the second phase itself when its amplitude is increased further, thereby offsetting its cancellation effect. We also tested a hypothesis that bipolar cancellation results from different spectral frequency content of uni- and bipolar pulses[20], but could not confirm it. Some observed peculiarities, such as positive correlation of bipolar cancellation with the cumulative duration of all nsEP applied, have yet to be explained.

2. Materials and Methods

2.1. Cells lines and media

Chinese hamster ovary cells (CHO-K1) and human monocyte lymphoma cells (U937) were purchased from the American Type Culture Collection (ATCC, Manassas, VA). CHO cells were propagated in Ham’s F12K medium (Mediatech Cellgro, Herdon, VA) supplemented

with 10% fetal bovine serum (FBS; Life Technologies, Grand Island, NY). U937 cells were cultured in RPMI-1640 medium (Sigma-Aldrich, St. Louis, MO) supplemented with 10 % FBS. Both cell lines were cultured at 37 °C with 5% CO_2 in air, and 100 I.U./ml penicillin and 0.1 μg/ml streptomycin (Mediatech Cellgro, Herdon, VA) were added to culture media to prevent contamination. Approximately one day prior to experiments, cells were seeded on glass coverslips coated with poly-L-lysine (Sigma-Aldrich) to improve cell adhesion. All experiments were performed at room temperature (22 ± 2°C).

2.2. Isolation and handling of adult murine VCM

All animal protocols were approved by the Institutional Animal Care and Use Committee, and experiments were performed in accordance with relevant guidelines and regulations. All chemicals, except for those labeled otherwise, were from Sigma-Aldrich. VCM from 3 to 5 month old DBA/2J female mice were isolated by Langendorff perfusion following protocols by Louch et al [21] with modifications. Mice were injected i.p. with with 0.5 cc heparin diluted in phosphate buffered saline (PBS) to 100 IU/ml and anesthetized by inhalation of 2-4% isoflurane in O_2. The heart was quickly excised and arrested in ice-cold mouse perfusion buffer gassed with 95% O_2/5% CO_2. The buffer containing (in mM): 113 NaCl, 4.7 KCl, 1.2 $MgSO_4$, 0.6 Na_2HPO_4, 0.6 KH_2PO_4, 12 $NaHCO_3$, 10 $KHCO_3$, 30 Taurine, 5.5 Glucose, 10 2,3-Butanedione monoxime, 10 HEPES (pH 7.4). Aorta was cannulated and the heart was retrogradely perfused using a two channels syringe pump (Harvard Apparatus, Cambridge, MA) to maintain a stable flow rate of 3 ml/min. Perfusion solution was heated to 37°C using a rod in-line heater connected to a TC-344B control unit (Warner Instruments, Hamden, CT). Temperature was monitored by a digital thermometer BAT-12 (Physitemp Clifton, NJ). Hearts were perfused for 4 min with the perfusion buffer and then for 8 min with digestion buffer (same formulation, but supplemented with 0.1 mg/ml Liberase TM (cat.# 05401127001, Roche, Switzerland) and 12.5 μM $CaCl_2$). Next, heart was taken off from the cannula, placed in a 35-mm culture dish with 3 ml of the digestion buffer and moved to a sterile laminar flow hood. Atria were removed, and ventricles were pulled apart with forceps, minced, and then gently triturated with a transfer pipette for 5 min. VCM suspension was filtered through a 100 μm cell strainer into a 50 ml tube and digestion was halted by adding 3 ml of perfusion buffer with 2 mg/ml of bovine serum albumin (BSA) fraction V and 12.5 μM $CaCl_2$. Cells were left to settle down for 15 min, and the supernatant was replaced with 10 ml of perfusion buffer with 1 mg/ml of BSA fraction V and 12.5 μM $CaCl_2$. Next, Ca^{2+} concentration was increased in several steps. First, two 50-μl aliquots of 10 mM $CaCl_2$ were added to the tube with cells with a 4-min interval. In 7-8 min after the second addition, supernatant was removed and replaced with 10 ml of control buffer containing (in mM): 133.5 NaCl, 4 KCl, 1.2 $MgSO_4$, 1.2 NaH_2PO_4, 11 Glucose, 10 HEPES; and 0.1% BSA (pH 7.4), supplemented with 200 μM $CaCl_2$. This procedure was repeated two more times, raising $CaCl_2$ concentration to 500 and 1,000 μM, with the same time intervals. Cells were seeded on laminin-coated 10 mm glass cover slips, and in 3 hours the medium was replaced with the incubation buffer of the same composition, but supplemented with 1 mM $CaCl_2$, 1% of 100× penicillin/streptomycin (Corning, Corning, NY), and 1% of 100X insulin-transferrin-selenium (Gibco, Gaithersburg, MD). Cell were kept at room temperature and typically used in experiments within 48 hr.

2.2 Evaluation of membrane permeabilization by fluorescence imaging

Procedures for measuring membrane permeabilization by YP uptake were similar to those described previously[4, 17, 22]. Briefly, a coverslip with attached cells was placed in a glass-bottomed chamber mounted on an Olympus IX81 inverted microscope equipped with an FV 1000 confocal laser scanning system (Olympus America, Center Valley, PA). For CHO and U037 cells, the chamber was filled with 0.35-0.4 ml of physiological solution containing (in mM): 140 NaCl, 5 KCl, 2 $CaCl_2$, 2 $MgCl_2$, 10 HEPES, and 10 Glucose (pH 7.4). For VCM, the solution contained 1 $CaCl_2$ and 1.5 $MgCl_2$; other components were the same. This solution was supplemented with one of the following fluorescent dyes: 1 μM of YP iodide (Thermo Fisher Scientific, Waltham, MA); 5 or 10 μg/ml of Pr iodide (Sigma-Aldrich); or Annexin V FITC (Thermo Fisher Scientific) at 1:50 dilution. YP and PR do not penetrate the intact cell membrane, and show essentially no fluorescence in the physiological solution. Once they enter the cell through a compromised membrane, they bind to nucleic acids and become brightly fluorescent. Both dyes are commonly used for detection of electroporation; YP is somewhat more sensitive but less specific (may pass through some endogenous channels) and is more prone to bleaching[17, 19, 23]. In contrast to YP and Pr, Annexin V FITC detects externalization of phosphatidylserine (PS) in response to electroporation (which may happen by either lateral drift through pores or by activation of scramblases by Ca^{2+} entry[22, 24, 25]).

In some experiments, $CaCl_2$ was omitted from the solution and replaced with 2 mM Na-EGTA. Since Annexin V binding to PS is Ca^{2+}-dependent, it cannot be used in a Ca^{2+}-free buffer; therefore we used instead a Ca^{2+}-independent bovine lactadherin-FITC (Hematologic Technologies, Essex, VT) at 1:30 dilution[24].

Differential-interference contrast (DIC) and fluorescent images were taken with a 40×, NA 0.95 dry objective. YP and Annexin V FITC (in different experiments) were excited with a 488 nm laser, and emission was detected between 505 and 525 nm. Pr was excited with 543 nm laser, and fluorescence was detected in the 560-660 nm range. The sensitivity of the emission detector (photomultiplier tube, PMT) was optimized for each set of experiments, in order to maximize the dynamic range while avoiding pixel saturation. The PMT setting were kept the same and constant throughout each set of experiments, but depending on the nsEP treatment (e.g., the number of pulses) could be set different for other sets. Hence, the arbitrary units (a.u.) across different sets of experiments were not necessarily the same, and quantitative comparisons, on many occasions, should be limited to within a particular set of experiments. In each set of experiments, different nsEP treatments were randomized with sham-exposed control experiments.

Images were taken every 10 s beginning before nsEP exposure, and continued as a time series for 3-5 min afterwards. Cells were exposed to nsEP at 28 or at 15 s from the onset of image acquisition to capture three or two baseline images prior to nsEP exposure. Image stacks were quantified using MetaMorph Advanced v.7.7.0.0 (Molecular Devices, Foster City, CA). For each cell, the average emission of the baseline images was subtracted from each acquired image; the baseline-subtracted fluorescence values were then plotted versus time.

2.3. nsEP Exposure

General methods of nsEP delivery to individual selected cells (or small groups of cells) on a microscope stage were described in detail previously [3, 17, 23]. A pair of tungsten rod electrodes (100 μm diameter, 140- to 300-μm gap) was connected to one of custom-made nsEP generators. Using an MPC-255 robotic manipulator (Sutter, Novato, CA), the electrodes were positioned within the microscope field of vision so that the selected cell was centered between the tips of the electrodes; then the electrodes were lifted to precisely 30 or 50 μm above the coverslip surface. Uninsulated tips of the electrodes remained fully submerged in the saline. VCM, which are large rod-shaped cells, were always oriented parallel to the electrodes (i.e., perpendicular to the electric field). U937 cells are essentially round; and CHO cells, which acquire random shapes, were not oriented in the electric field in any particular way.

Traces of various nsEP tested in this study are shown in Fig. 1. Trapezoidal pulses were produced by a MOSFET-based generator capable of delivery of uni- and bipolar pulses with variable duration and amplitude of each phase. The design and operation of this pulse generator have been reported in detail recently [26]. In brief, bipolar nsEP were generated using two separate high-voltage DC power supplies, charging capacitors of two channels of the nsEP generator to desired positive and negative potentials. The capacitors were turned on and off by a power MOSFET switch (IXYS, IXFB38N100Q2) for a given period of time, controlled with a digital delay generator (model 577-8C, Berkeley Nucleonics Corporation, San Rafael, CA). In turn, the delay generator was triggered and synchronized with image acquisitions by a TTL pulse protocol using Digidata 1440A board and Clampex v. 10.2 software (Molecular Devices, Sunnyvale, CA). The nsEP repetition rate, the number of nsEP, and the synchronization of nsEP exposure with image acquisitions were all programmed in pClamp. Over the course of experiments, we used two different modifications of the MOSFET-based pulse generator, which explains slightly different pulse shapes in panel A versus panels C and D of Fig. 1.

In different sets of experiments, we tested uni- and bipolar trapezoidal nsEP with a phase duration of 200, 230, and 800 ns (Fig.1). The maximum amplitude of each phase was limited by the output of pulse generator to about 800 V, which translated into 30 kV/cm at the cell location. In order to produce quantifiable bioeffects, we usually had to deliver multiple nsEP. The treatment parameters tested in each set of experiment are provided in full (type of pulses, their number, duration, electric field strength, and repetition rate) with the description of this experiment in figures and figure captions.

Nanosecond electric field oscillation (NEFO; Fig. 1B) were produced by solid-state pulse generators described in detail previously [4]. The unipolar NEFO was obtained by rectifying a damped sine wave waveform. The duration of each phase of the pulse and the ratio of amplitudes of the first and second phases were preset in each NEFO generator, and could not be adjusted by user. In this study, we used bipolar, multiphasic NEFO with the second phase tuned to 23% and 61% of the first phase (referred to as B_{23} and B_{61}). The width of the first phase at 50% height was 236 ns for both the unipolar NEFO and B_{23}, but was reduced to 186 ns for B_{61} (the increase of the 2nd phase caused inevitable shortening of the first phase). The energy delivered into a resistive load by bipolar NEFO was 15% (B_{23}) and 41% (B_{61})

larger than by the unipolar NEFO with the same amplitude of the 1st phase, despite the phase width reduction in B_{61}. NEFO were triggered directly from Digidata as described above, without a delay generator.

NEFO waveforms were tested in two sets of experiments, to study the effect of the reversal polarity phase on YP uptake in CHO cells and on phosphatidylserine externalization in U937 cells. The maximum amplitude of NEFO (about 300 V at the peak of the first phase) was limited by the NEFO generator capabilities. Even at the maximum output, we needed to deliver multiple NEFO to produce quantifiable effects. NEFO parameters tested in specific experiments are provided in respective figures and figure captions.

Hereinafter in this paper, the reported pulse amplitude and the electric field intensity are those at the peak of the first phase of the pulse. The electric field at the cell location was determined in a manner similar to what was described previously [17, 18] by 3D numerical simulations using a commercial finite element solver COMSOL Multiphysics, Release 5.0 (Stockholm, Sweden). The exact shape and amplitude of nsEP were monitored using a TDS 3052B oscilloscope (Tektronix, Beaverton, OR). In all experiments, each cell or group of cells was subjected to nsEP exposure only once.

2.4. General Protocols and Statistics

All experiments were designed to minimize potential biases and to ensure the accuracy and reproducibility of results. All experiments included sham-exposed parallel control groups, in which cells were subjected to all the same manipulations and procedures except the nsEP exposure itself (i.e., equivalent to an nsEP exposure at zero pulse amplitude). Various protocols of nsEP treatments and parallel control experiments were alternated in a random manner. The number of cells exposed to nsEP in a single experiment varied for different cell types: We exposed clusters of 3-6 CHO cells at a time, but only 1 or 2 U937 cells, and always a single VCM at a time. The number of cells used for statistical analysis for each type of treatment is indicated in figure captions. Student's *t*-test with Dunnet's correction when applicable[27, 28] was employed to analyze the significance of differences. Data are presented in graphs as mean values +/− s.e. for *n* independent experiments; $p < 0.05$ (2-tailed) was considered statistically significant. Due to multiple statistical comparisons made between different groups we chose to let the error bars speak for the statistical difference, with a pertinent notion in the caption (such as "Non-overlapping error bars indicate statistically significant difference at $p<0.05$ or better ") while minimizing the use of special symbols.

3. Results

3.1 Bipolar cancellation of YP uptake in CHO cells

Initiation of YP uptake by nsEP and its cancellation by reversing pulse polarity has been shown for symmetrical nsEP with various phase separations[3], for non-symmetrical nsEP with different duration of the first and the second phases[16], and for NEFO with a second phase fixed at 35% of the first one[4]. Here, we specifically test how the ratio of the opposite polarity phase affects cancellation.

In the first set of experiments, we used 230-ns trapezoidal pulses shown in Fig.1A. The amplitude of the 2nd phase was set at 0% (unipolar pulse), 20%, 50%, or 100% of the first phase. A train of 4 such nsEP at 9 kV/cm, 2 Hz triggered immediate dye entry, which slowed down gradually during 5 min of observation (Fig. 2A). The unipolar pulse caused the strongest membrane permeabilization; adding a 20% second phase reduced the effect already by 30% ($p<0.05$), and a 50% second phase reduced the effect more than 2-fold ($p<0.01$). Unexpectedly, further increase of the second phase to 100% did not facilitate cancellation beyond what was already accomplished with the 50% 2nd phase.

The same trend, along with a somewhat stronger cancellation was observed when permeabilizing CHO cells with NEFO (10 pulses, 2 Hz, 7.2 kV/cm). The effect of unipolar NEFO was decreased almost twofold by B_{23} and as much as tenfold by B_{61} ($p<0.01$, Fig. 2B). However, it is possible that the reduced width of the first phase in B_{61} (see section 2.3) also contributed to the reduced effect.

3.2 Bipolar cancellation of PS externalization in U937 cells

Round-shaped cells like U937 are particularly useful to study the localization of electroporative membrane damage with respect to nsEP-delivering electrodes. Maximum electroporation occurs at cell poles facing the electrodes. It is commonly seen that more damage occurs at the anode-facing pole [23], and one might expect that switching the anode and cathode positions (i.e., by changing the polarity of the pulse) should cause damage on both sides of the cell. A train of 50 unipolar NEFO (5 Hz, 10 kV/cm) caused gradually increasing PS externalization, with larger effect at the anode-facing pole of the cell (Fig. 3). Such unipolar NEFO treatment also caused cell swelling and blebbing (bulging of the plasma membrane; Fig. 3, inset). B_{23} had a twofold smaller effect on PS externalization, whereas B_{61} caused no effects (Fig. 3). B_{23} reduced the difference between PS externalization at the anode- and cathode-facing poles of the cell (Fig. 3C), which matches independent observations using symmetrical and asymmetrical trapezoidal bipolar nsEP[16]. The asymmetry of response to B_{61} could not be measured due to the lack of any effect.

In a separate set of experiments, we showed that the same trains of NEFO caused no PS externalization in a Ca^{2+}-free solution (data not shown). This result points at the involvement of scramblases, Ca^{2+}-dependent enzymes which destroy the phospholipid asymmetry of cell plasma membrane [4]. It suggests that the reduced PS externalization by bipolar NEFO was a downstream effect of bipolar cancellation of Ca^{2+} entry, the effect that was demonstrated earlier for trapezoidal bipolar pulses[2].

3.3 Bipolar cancellation of Pr uptake in VCM depends on pulse duration and pulse number

Primary VCM are different morphologically and physiologically from cultured cell lines, which could affect their sensitivity to nsEP. They are large rod-shaped cells, 20-40 μm wide and often over 100 μm long; they have rough edges and relatively flat top surface (Fig. 4A; compare with insets in Figs. 2 and 3). This is the first time when bipolar pulses were tested in VCM. Membrane permeabilization was quantified by Pr uptake for two pulse durations (200 and 830 ns at 50% height) and for different numbers of pulses (from 1 to 20); the pulse repetition rate and amplitude were kept constant at 5 Hz and 800 V (which produced 30

kV/cm field at cell location. For bipolar pulses, the second phase of the opposite polarity had the same amplitude and duration as the first phase.

A single 200-ns pulse caused just a marginally detectable Pr uptake, without any sign of bipolar cancellation (Fig. 4B, left panel). Applying two or more pulses expectedly caused more Pr uptake and, concurrently, the difference between unipolar and bipolar pulses increased and became statistically significant at $p<0.01$ for 10- and 20-pulse trains (Fig. 4B).

With 830-ns pulses, a single uni- and bipolar pulse produced similar effects, but the difference between uni- and bipolar pulses became significant at $p<0.02$ already with 5 pulses and increased further for longer trains (Fig. 4C). These data contrasted our earlier findings of YP uptake in NEFO-exposed CHO cells, which showed no dependence of bipolar cancellation on the number of NEFO applied[4]. For VCM, the difference in Pr uptake caused by uni- and bipolar pulses (as measured at 300 s, data from Fig. 4) increased proportionally to the number of pulses as a logarithmic function (Fig. 5A). The slope of the best fit function was the same for 200- and 830-ns pulses, but with a vertical shift. This observation prompted us to take the pulse duration into account, by plotting the data for longer pulses against a separate X-axis and shift it so that a single 830+830 ns pulse would correspond to 4.15 of 200+200 ns pulses (Fig. 5B). The result was equivalent to plotting the data against the cumulative duration of all pulses applied, and all the datapoints could be fitted well with one logarithmic function (Fig 5C; best fit $R^2=0.88$).

The only explanation to this dependence is that having nsEP “on” changes VCM sensitivity to nsEP, and does it differently for uni- and bipolar pulses. One possibility is that cells exposed to unipolar nsEP become more vulnerable to the next unipolar nsEP, whereas bipolar nsEP have little effect on sensitivity. Alternatively, it could be bipolar nsEP which decrease the sensitivity to the next bipolar nsEP, whereas unipolar pulses have little impact. In either scenario, this behavior resembles the effect of electrosensitization[29–32], an electroporation-induced hypersensitivity to subsequent electroporation treatments, which develops within seconds or tens of seconds after the first nsEP delivery. Electrosensitization increases when pulses are delivered at longer intervals, i.e., when the pulse repetition rate is low enough[29,32]. Therefore, we tested if delivering the same train of 10 pulses at 0.5, 2, or 5 Hz might affect the bipolar cancellation. Contrary to the expectations, the efficiency of bipolar 200+200 ns pulses stayed at about 50% of the effect of 200-ns unipolar pulses regardless of the repetition rate (Fig. 5D).

3.4 Impact of the 2nd phase amplitude on bipolar cancellation of PR uptake in VCM

We performed these experiments using trains of 10, 830-ns pulses, because of robust bipolar cancellation observed with these treatment parameters (Fig. 4C). The amplitude of the first phase was kept constant at 400 V (15 kV/cm), whereas the amplitude of the second phase was varied from 200 to 800V (7.5 to 30 kV/cm). Unexpectedly, it was the smallest second phase (200 V, 50% of the first one) which caused maximum cancellation and minimum Pr uptake (Fig. 6A). Increasing the 2nd phase to 400 and 600 V (100% and 150% of the first phase) still caused less Pr uptake than a unipolar 400 V pulse, i.e., still caused cancellation. However, making the 2nd phase even larger (800 V or 200%) started to incur more membrane damage than a single unipolar pulse. Strong cancellation by the asymmetrical

pulse with a 50% smaller 2nd phase was preserved when the amplitude of the pulse was doubled to 800 V (Fig. 6B).

A similar set of experiments was performed using trains of 10, 200-ns pulses. The first phase was kept constant at 800 V (30 kV/cm), and the second phase was varied from 200 to 800V (7.5 to 30 kV/cm). We could not go beyond 800 V, which was close to the limit of our nsEP generator, but explored the lower range of the 2nd phase amplitudes in more detail. Same as with the longer pulses, the Pr uptake was minimal when the 2nd phase was at 400V, or 50% of the 1st one (Fig. 6C). Either decreasing the second phase to 200V or increasing it to 600V and 800V weakened cancellation, but all these treatments caused significantly less Pr uptake than a unipolar 800 V, 200 ns pulse.

3.5 The efficiency of an asymmetric bipolar pulse depends on the sequence of smaller and larger phases

A recent study attributed the phenomenon of bipolar cancellation to different low frequency content in uni- and bipolar nsEP [20]. Indeed, the electroporation efficiency of diverse bipolar pulses, including different delays between the two phases, correlated with the low-frequency spectral content; however, it remained unclear if the low frequencies are critical for electroporation, or the observed correlation just reflects the fact that uni- and bipolar pulses have different frequency spectra. To test it out, in Fig. 6B we specifically compared the biological efficiency of two different bipolar pulses having the same spectral frequency content. The pulses consisted of two identical phases presented in different sequence, 400V + 800V and 800V + 400V. Experiments established profoundly different efficiency of this pulses, i.e., 800 V + 400 V treatment caused almost 3-fold less Pr uptake ($p<0.01$) than its “mirror reflection” 400 V + 800 V pulse. Thus the hypothesis about the role of nsEP frequency content for bipolar cancellation could not be confirmed. In addition, it is worth noting that 800V + 400V pulses were less efficient than unipolar pulses of only 400V ($p<0.05$), despite delivering 5-fold more energy into the sample.

4. Discussion

Our experiments demonstrated that bipolar cancellation of electroporation is common for diverse cell types and for various endpoints, using various shapes and configurations of nsEP. Our study was focused primarily on the role of the amplitude of the second phase of nsEP, and quantitative results from all series of experiments performed are summarized in Fig. 7. Each panel of this figure represents one or several sets of experiments described above, and the degree of bipolar cancellation is evaluated as a ratio of bi- and unipolar pulse effects, as measured by the end of the experiment (200 s for panel B and 300 s for other panels).

One new and unexpected conclusion from these data is that maximum bipolar cancellation consistently develops with the second phase of the pulse being about 2-fold smaller than the first phase. A smaller first phase caused less cancellation, and a larger second phase either did not cause more cancellation (Fig. 7A), or reduced it (Fig. 7D). Moreover, a bipolar pulse with a too large second phase could produce more electroporation than a unipolar pulse (Fig7D, 830 ns and Fig. 6A, 400V+800V). This behavior is very logical, taking into account

that the 2nd phase not only cancels the effect of the first one, but has electroporating effect of its own. The overall effect is a result of summation of the two; for example, in a 400V+800V bipolar pulse, the second phase still cancels the effect of the first phase, but at the same time causes strong electroporation which offsets its protective effect. With the second phase of about 50% of the first phase, its canceling effect is already strong, whereas its electroporative effect is still weak; that is why the effect of the bipolar pulse is at its minimum.

Importantly, it is not just the 2nd phase that cancels the effect of the first one. The first phase itself reduces the membrane injury by the 2nd phase, making it less efficient. This is precisely the reason why a symmetrical bipolar pulse is less efficient than either of its phases applied as separate unipolar pulses. Likewise, it explains why the 400V+800V bipolar pulse in Fig. 6B is less efficient than the 800V pulse alone. The fact that switching the sequence of two phases of a bipolar pulse (compare 400V+800V and 800V+400V, Fig. 6B) has a major impact on its electroporation efficiency indicates that “canceling” effect of the second phase is much stronger than the reciprocal inhibitory effect of the first phase on the second one.

A similar interplay of two phases was noted when varying each phase duration while keeping their amplitude the same[16]: A bipolar pulse composed of a 300ns + 900ns pulse caused 2-fold more YP uptake than 900ns+300ns. Delivering a more “intense” second phase (having higher amplitude or longer duration) after a “weaker” first phase always caused stronger overall effect than the reverse sequence of phases. Of note, the temporal sequence of the “weaker” and “stronger” phases of a bipolar pulses does not change its spectral frequency content. Therefore the profoundly different effect of such pulses indicate that the spectral frequency content is not the cause of bipolar cancellation, as was hypothesized previously[20].

The data in Fig. 7D show some remarkable similarities between nsEP of different duration and amplitude. Indeed, reducing pulse duration from 830 to 200 ns and/or increasing its amplitude 2-fold had little or no impact on the degree of bipolar cancellation. The lack of the effect of pulse amplitude is consistent with earlier studies of bipolar cancellation by NEFO[4]. However, in some other experiments with NEFO and measuring YP uptake, we observed weakening of bipolar cancellation with more intense electric field (unpublished). One may also note stronger bipolar cancellation by NEFO (Fig. 7B,C) than by trapezoidal pulses (Fig. 7A,D); however this result could be affected by the reduced width of bipolar NEFO (see Fig. 1) and remains to be confirmed.

At present, the phenomenon of bipolar cancellation poses more questions than gives answers. Thus far, its underlying mechanism could not be explained within the framework of existing concepts of nanoelectroporation. To identify this mechanism, it may be critical to test in future studies if bipolar cancellation takes place in cell-free systems (e.g., giant unilamellar vesicles and lipid bilayers) or is restricted to biological membrane structures.

Acknowledgments

The study was supported by an AFOSR MURI grant FA9550-15-1-0517 (to AGP) on Nanoelectropulse-Induced Electromechanical Signaling and Control of Biological Systems, administered through Old Dominion University, and by R01HL128381 from NHLBI (to AGP).

References

1. Ibey BL, Ullery JC, Pakhomova ON, Roth CC, Semenov I, Beier HT, Tarango M, Xiao S, Schoenbach KH, Pakhomov AG. Bipolar nanosecond electric pulses are less efficient at electropermeabilization and killing cells than monopolar pulses. Biochem Biophys Res Commun. 2014; 443:568–573. [PubMed: 24332942]
2. Pakhomov AG, Semenov I, Xiao S, Pakhomova ON, Gregory B, Schoenbach KH, Ullery JC, Beier HT, Rajulapati SR, Ibey BL. Cancellation of cellular responses to nanoelectroporation by reversing the stimulus polarity. Cell Mol Life Sci. 2014; 71:4431–4441. [PubMed: 24748074]
3. Gianulis EC, Casciola M, Xiao S, Pakhomova ON, Pakhomov AG. Electropermeabilization by uni- or bipolar nanosecond electric pulses: The impact of extracellular conductivity. Bioelectrochemistry. 2017; 119:10–19. [PubMed: 28865240]
4. Gianulis EC, Lee J, Jiang C, Xiao S, Ibey BL, Pakhomov AG. Electroporation of mammalian cells by nanosecond electric field oscillations and its inhibition by the electric field reversal. Sci Rep. 2015; 5:13818. [PubMed: 26348662]
5. Pakhomova ON, Gregory B, Semenov I, Pakhomov AG. Calcium-mediated pore expansion and cell death following nanoelectroporation. Biochim Biophys Acta. 2014; 1838:2547–2554. [PubMed: 24978108]
6. Kotnik T, Pucihar G, Rebersek M, Miklavcic D, Mir LM. Role of pulse shape in cell membrane electropermeabilization. Biochim Biophys Acta. 2003; 1614:193–200. [PubMed: 12896812]
7. Kotnik T, Mir LM, Flisar K, Puc M, Miklavcic D. Cell membrane electropermeabilization by symmetrical bipolar rectangular pulses. Part I. Increased efficiency of permeabilization. Bioelectrochemistry. 2001; 54:83–90. [PubMed: 11506978]
8. Kotnik T, Miklavcic D, Mir LM. Cell membrane electropermeabilization by symmetrical bipolar rectangular pulses. Part II. Reduced electrolytic contamination. Bioelectrochemistry. 2001; 54:91–95. [PubMed: 11506979]
9. Tekle E, Astumian RD, Chock PB. Electroporation by Using Bipolar Oscillating Electric-Field - an Improved Method for DNA Transfection of Nih 3t3 Cells. P Natl Acad Sci USA. 1991; 88:4230–4234.
10. Tovar O, Tung L. Electroporation of Cardiac Cell-Membranes with Monophasic or Biphasic Rectangular Pulses. Pace. 1991; 14:1887–1892. [PubMed: 1721194]
11. Faurie C, Rebersek M, Golzio M, Kanduser M, Escoffre JM, Pavlin M, Teissie J, Miklavcic D, Rols MP. Electro-mediated gene transfer and expression are controlled by the life-time of DNA/membrane complex formation. J Gene Med. 2010; 12:117–125. [PubMed: 19941315]
12. Faurie C, Phez E, Golzio M, Vossen C, Lesbordes JC, Delteil C, Teissie J, Rols MP. Effect of electric field vectoriality on electrically mediated gene delivery in mammalian cells. Biochim Biophys Acta. 2004; 1665:92–100. [PubMed: 15471575]
13. de Oliveira PX, Bassani RA, Bassani JW. Lethal effect of electric fields on isolated ventricular myocytes. IEEE Trans Biomed Eng. 2008; 55:2635–2642. [PubMed: 18990634]
14. Esser AT, Smith KC, Gowrishankar TR, Vasilkoski Z, Weaver JC. Mechanisms for the intracellular manipulation of organelles by conventional electroporation. Biophys J. 2010; 98:2506–2514. [PubMed: 20513394]
15. Schoenbach KH, Pakhomov AG, Semenov I, Xiao S, Pakhomova ON, Ibey BL. Ion transport into cells exposed to monopolar and bipolar nanosecond pulses. Bioelectrochemistry. 2015; 103:44–51. [PubMed: 25212701]
16. Valdez CM, Barnes RA Jr, Roth CC, Moen EK, Throckmorton GA, Ibey BL. Asymmetrical bipolar nanosecond electric pulse widths modify bipolar cancellation. Sci Rep. 2017; 7:16372. [PubMed: 29180756]

17. Pakhomov AG, Gianulis E, Vernier PT, Semenov I, Xiao S, Pakhomova ON. Multiple nanosecond electric pulses increase the number but not the size of long-lived nanopores in the cell membrane. Biochim Biophys Acta. 2015; 1848:958–966. [PubMed: 25585279]
18. Gianulis EC, Pakhomov AG. Gadolinium modifies the cell membrane to inhibit permeabilization by nanosecond electric pulses. Arch Biochem Biophys. 2015; 570:1–7. [PubMed: 25707556]
19. Sozer EB, Levine ZA, Vernier PT. Quantitative Limits on Small Molecule Transport via the Electropermeome - Measuring and Modeling Single Nanosecond Perturbations. Sci Rep. 2017; 7:57. [PubMed: 28246401]
20. Merla C, Pakhomov AG, Semenov I, Vernier PT. Frequency spectrum of induced transmembrane potential and permeabilization efficacy of bipolar electric pulses. Biochim Biophys Acta. 2017; 1859:1282–1290. [PubMed: 28432034]
21. Louch WE, Sheehan KA, Wolska BM. Methods in cardiomyocyte isolation, culture, and gene transfer. J Mol Cell Cardiol. 2011; 51:288–298. [PubMed: 21723873]
22. Pakhomov AG, Bowman AM, Ibey BL, Andre FM, Pakhomova ON, Schoenbach KH. Lipid nanopores can form a stable, ion channel-like conduction pathway in cell membrane. Biochem Biophys Res Commun. 2009; 385:181–186. [PubMed: 19450553]
23. Bowman AM, Nesin OM, Pakhomova ON, Pakhomov AG. Analysis of plasma membrane integrity by fluorescent detection of Tl(+) uptake. J Membr Biol. 2010; 236:15–26. [PubMed: 20623351]
24. Muratori C, Pakhomov AG, Gianulis E, Meads J, Casciola M, Mollica PA, Pakhomova ON. Activation of the phospholipid scramblase TMEM16F by nanosecond pulsed electric field (nsPEF) facilitates its diverse cytophysiological effects. J Biol Chem. 2017
25. Vernier PT, Sun Y, Marcu L, Craft CM, Gundersen MA. Nanoelectropulse-induced phosphatidylserine translocation. Biophys J. 2004; 86:4040–4048. [PubMed: 15189899]
26. Ryan HA, Hirakawa S, Yang E, Zhou C, Xiao S. High-Voltage, Multiphasic, Nanosecond Pulses to Modulate Cellular Responses. IEEE Transactions on biomedical circuits and systems. 2018:1–13. PP.
27. Dunnet CW. A multiple comparison procedure for comparing several treatments with a control. J of the American Statistical Association. 1955; 50:1096–1121.
28. Winer BJ. Statistical Principles in Experimental Design, McGraw-Hill Book Company, New York. 1971
29. Jensen SD, Khorokhorina VA, Muratori C, Pakhomov AG, Pakhomova ON. Delayed hypersensitivity to nanosecond pulsed electric field in electroporated cells. Sci Rep. 2017; 7:10992. [PubMed: 28887559]
30. Dermol, J., Pakhomova, ON., Xiao, S., Pakhomov, AG., Miklavčič, D. Cell Sensitization is Induced by a Wide Range of Permeabilizing Electric Fields. In: Jarm, T., Kramar, P., editors. 1st World Congress on Electroporation and Pulsed Electric Fields in Biology, Medicine and Food & Environmental Technologies. Springer; Singapore: 2016. p. 163-166.
31. Pakhomova ON, Gregory BW, Pakhomov AG. Facilitation of electroporative drug uptake and cell killing by electrosensitization. Journal of cellular and molecular medicine. 2013; 17:154–159. [PubMed: 23305510]
32. Pakhomova ON, Gregory BW, Khorokhorina VA, Bowman AM, Xiao S, Pakhomov AG. Electroporation-induced electrosensitization. PLoS One. 2011; 6:e17100. [PubMed: 21347394]

Highlights

- Bipolar cancellation is common for diverse cell types and pulsing protocols
- Cancellation was not much affected by the electric field, pulse rate or width
- The ratio of opposite polarity phases determines cancellation efficiency
- Peak cancellation is observed with the 2nd phase of about 50% of the 1st one
- Spectral content of pulses does not determine cancellation

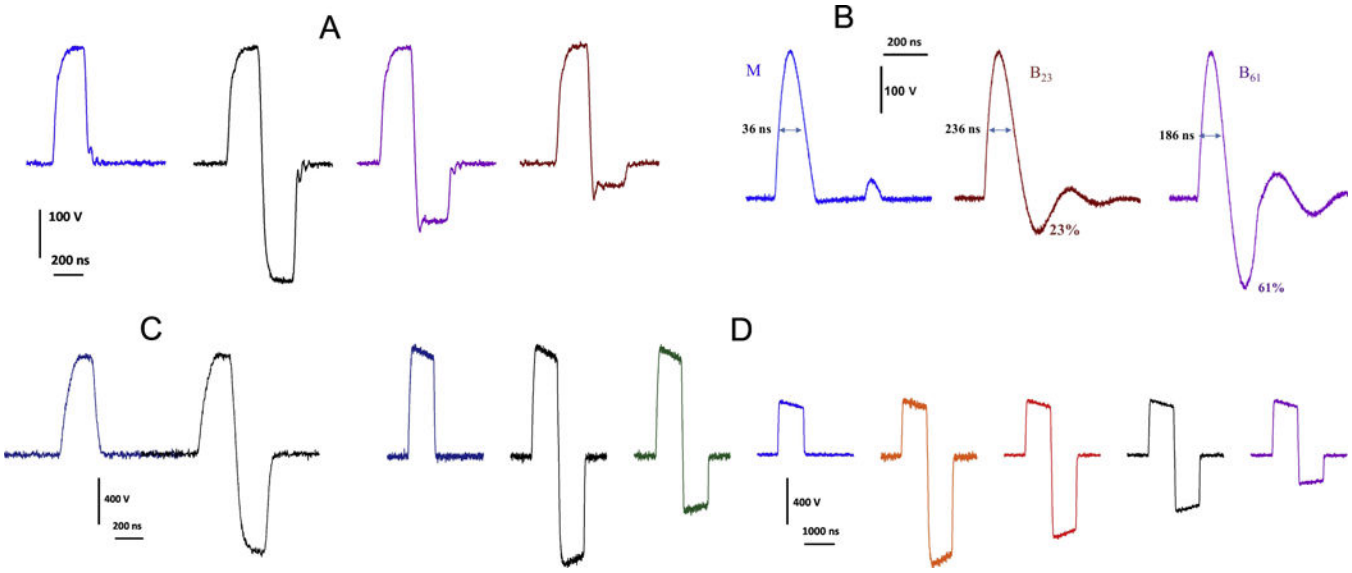

Fig. 1.

Representative traces of various uni- and bipolar nsEP tested in this study. A: trapezoidal pulses, 230 ns at 50% height, used for YP uptake measurements in CHO cells (Fig. 2A). B: nanosecond electric field oscillations (NEFO), used for YP uptake measurements in CHO cells (Fig. 2B) and phosphatidylserine externalization measurements in U937 cells (Fig. 3). Bipolar NEFO with the 2nd phase amplitude of 23% and 61% of the first phase are referred to as B_{23} and B_{61}, respectively. C and D are trapezoidal pulses which were used in experiments with VCM (Figs. 3–6); their width at 50% height was 200 ns (C) and 830 ns (D).

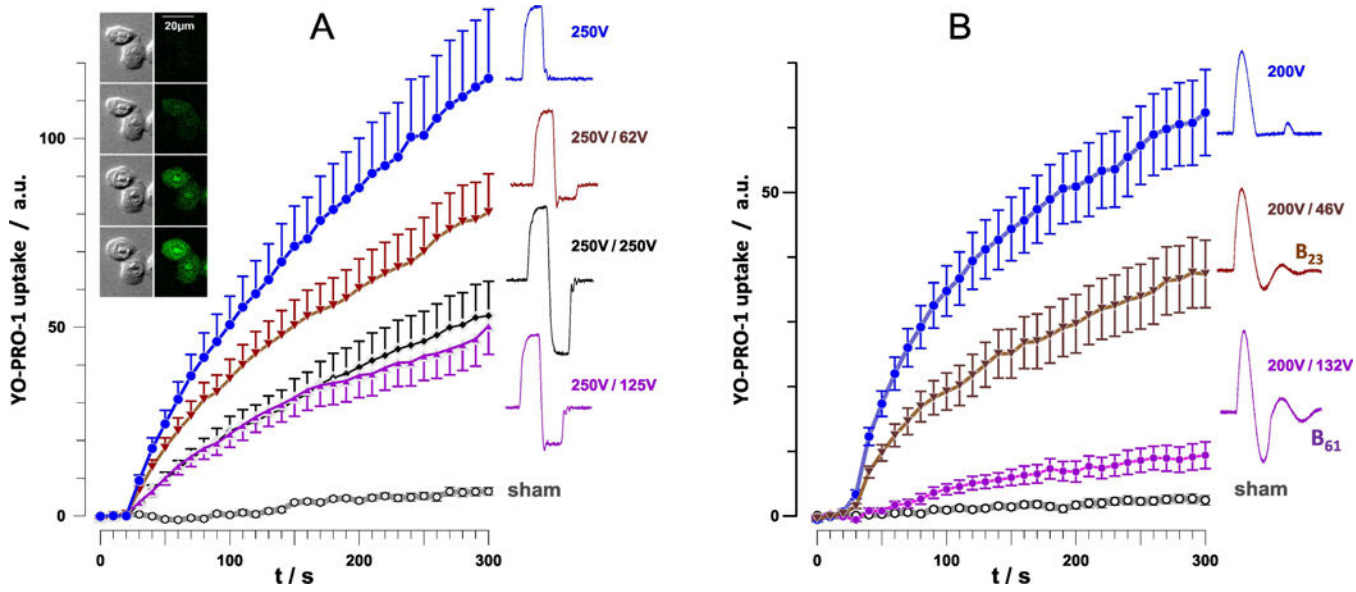

Fig. 2.

Time course of YP uptake in CHO cells after permeabilization by trapezoidal nsEP (A) and NEFO (B). Cells were exposed starting at 28 s into the experiment to a train of 4 pulses at 9 kV/cm, 2 Hz, 230 ns phase duration (A) or to a train of 10 NEFO (unipolar, B_{23}, and B_{61}) at 7 kV/cm, 2 Hz (B); see text and Fig.1 for more details. nsEP and NEFO shapes and voltages of the 1st and 2nd phases are provided next to the plots. Mean +/s.e. for n=17-23 (A) or n=20-40 (B). All bipolar pulse treatments caused significantly less membrane permeabilization than unipolar pulses ($p<0.01$). The inset shows representative DIC (left column) and YP fluorescence images at 0, 60, 180, and 300 s (from top to bottom). The cells were exposed to 4 unipolar, 230 ns, 9 kV/cm nsEP at 28 s.

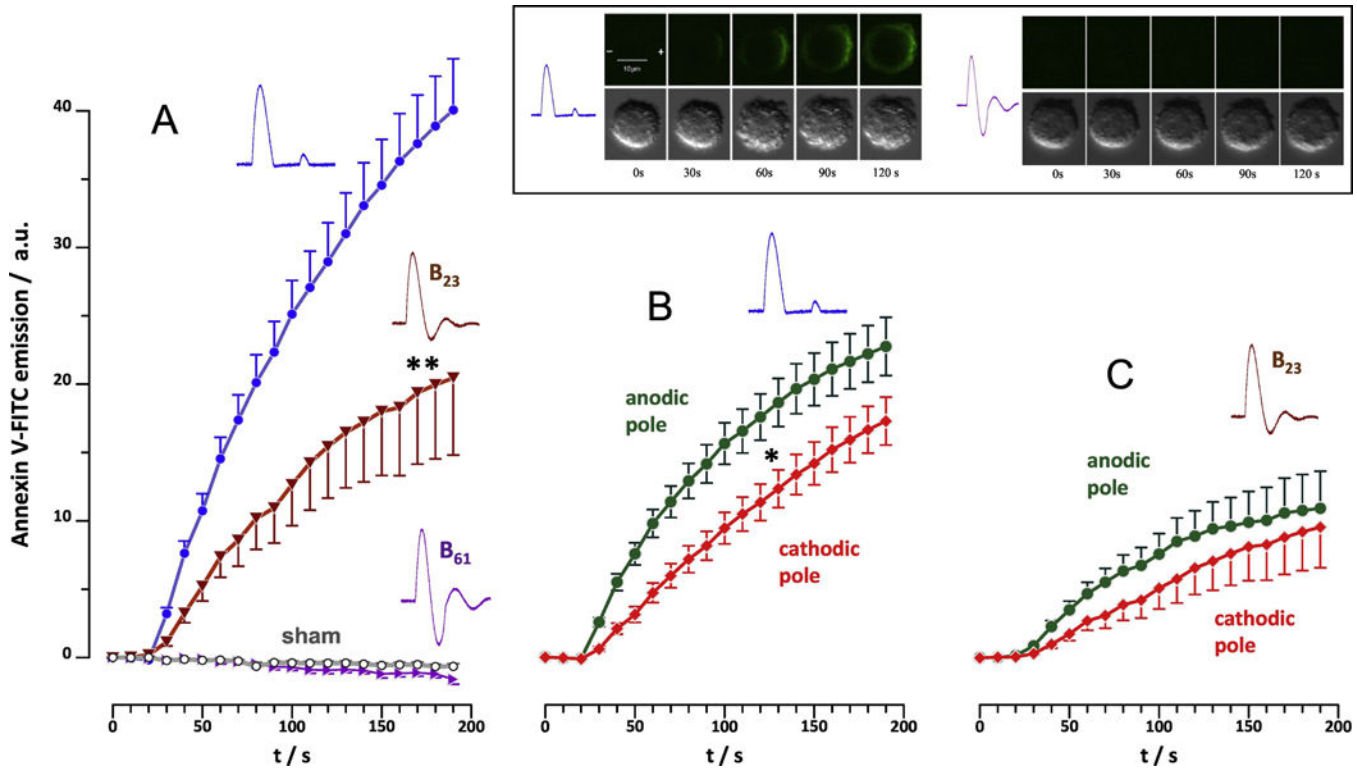

Fig. 3.

Phosphatidylserine externalization in U937 cells following exposure to 50 NEFO (unipolar, B23, or B61), 5 Hz, 10 kV/cm, starting at 15 s. Externalization was measured as a gain in Annexin V-FITC emission averaged over the entire cell (A) or separately for anode- and cathode-facing hemispheres (B for unipolar NEFO and C for B_{23}). Note the lack of any response to B_{61} (A). Mean +/s.e. for n=26-42. * $p<0.5$ for the difference between anodic and cathodic poles; ** $p<0.01$ for the difference of B_{23} from unipolar NEFO. The inset shows representative time course of PS externalization after unipolar NEFO (left panels) and the lack of detectable effects after B_{61} (right). Top: Annexin V-FITC emission; bottom: DIC images. The top left panel also shows directions to anode (+) and cathode (−).

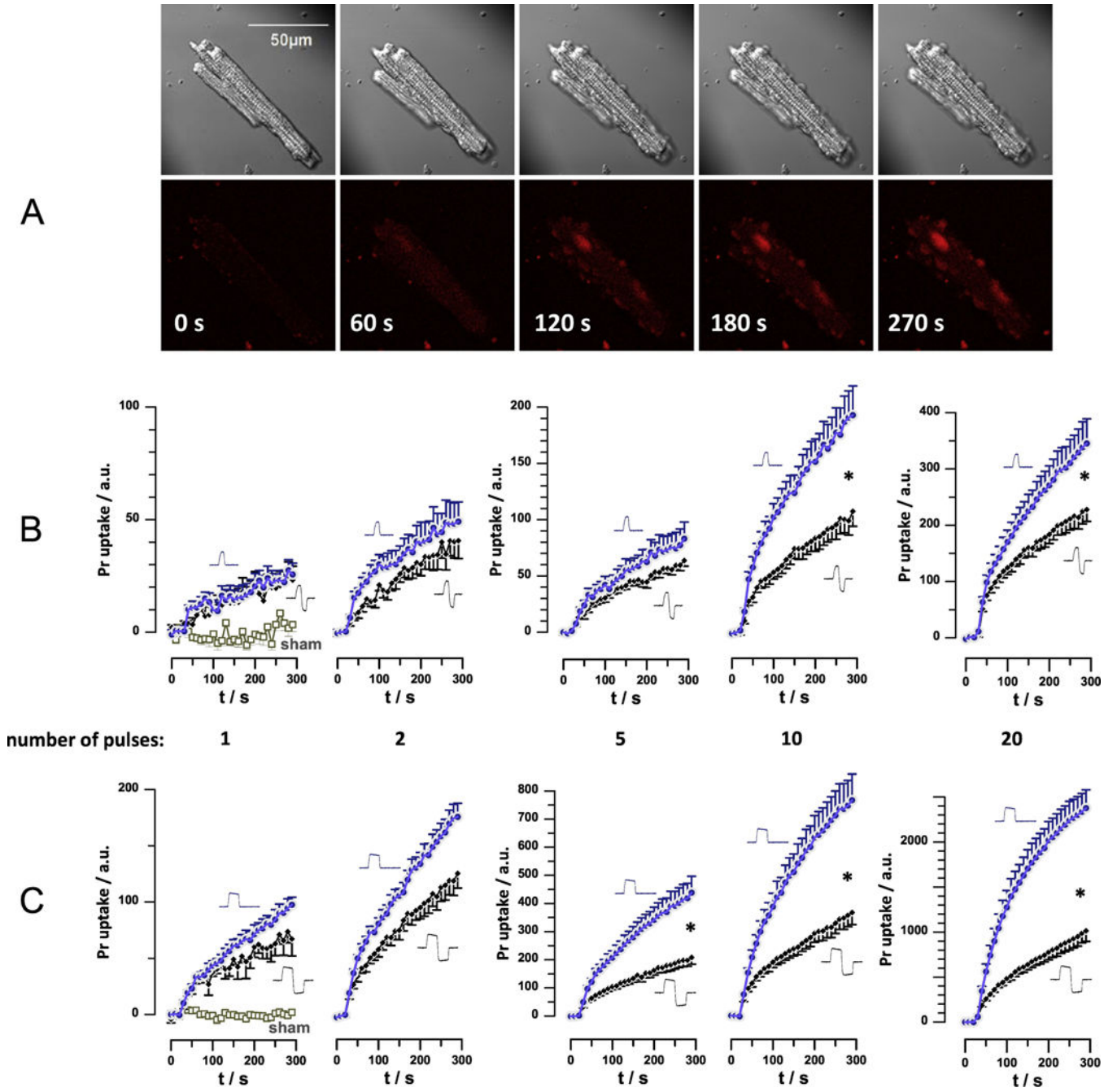

Fig. 4.

Bipolar cancellation of Pr uptake in primary ventricular cardiomyocytes (VCM). A: Representative time lapse images of a mouse VCM exposed to 10, 200-ns unipolar nsEP (30 kV/cm, 5 Hz), starting at 10 s into experiment. Dark shadows in diagonal corners of DIC images (top row) are those of nsEP-delivering electrodes. Bottom row: Pr fluorescence and time stamps. B: Time course of Pr fluorescence in VCM subjected to 200-ns unipolar or 200+200 ns symmetrical bipolar nsEP. The pulse amplitude and delivery rate was kept constant at 800 V (producing 30 kV/cm) and 5 Hz. The number of pulses was varied from 1 to 20 and is indicated under the graphs. The plots for uni- and bipolar pulses are identified

by pulse shapes next to the graphs. Data for sham exposure are shown in the left panel only and apply to all experiments. C: same as B, but for 800 ns unipolar and 800+800 ns bipolar nsEP. Mean +/− s.e,, n= 9-11. For clarity, error bars are shown in one direction only; * designates significant difference between uni- and bipolar pulse effects, at $p<0.05$ or better. Arbitrary units (a.u.) for Pr emission are the same for all panels; note different scales for Y-axes.

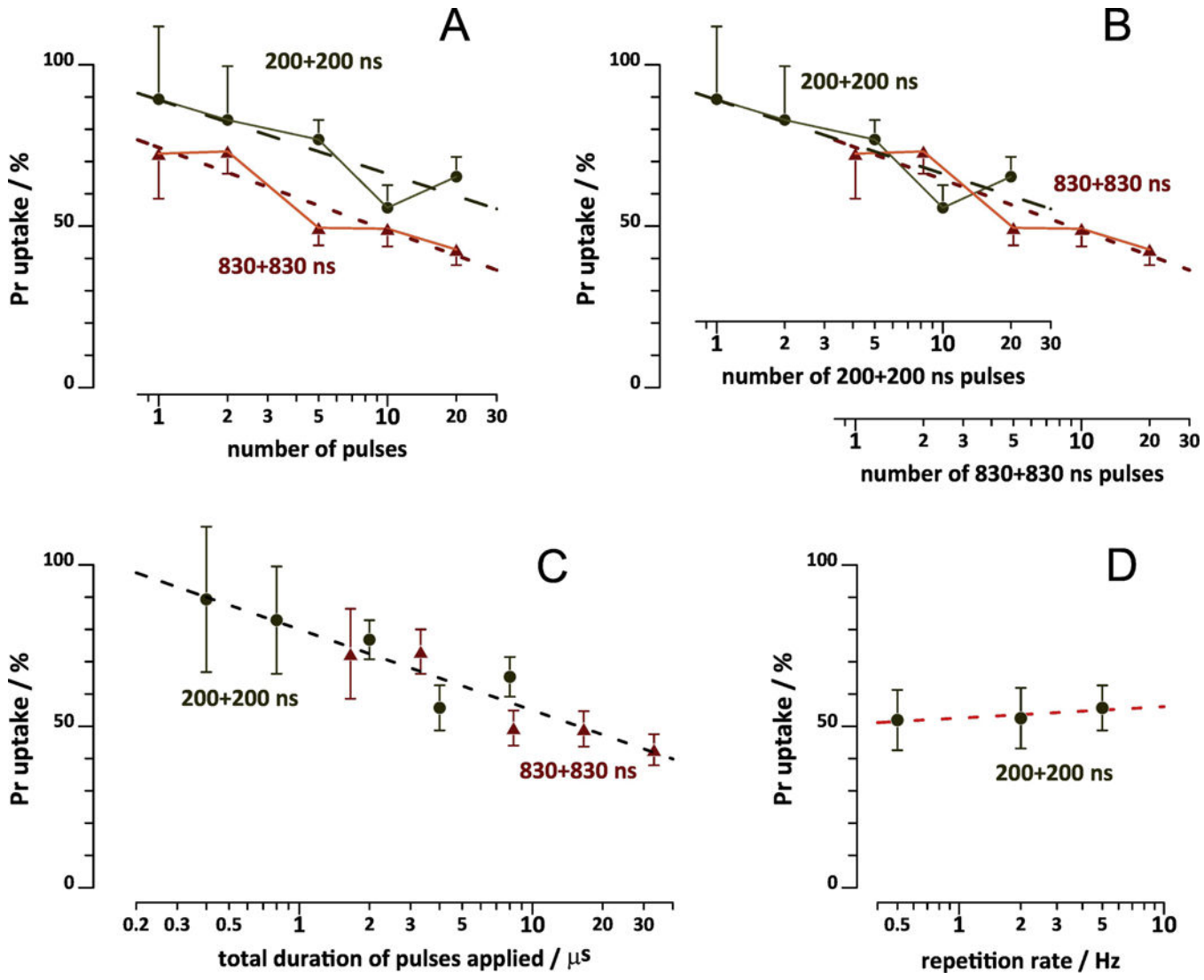

Fig. 5.

Effect of pulse number (A-C) and pulse repetition rate (D) on bipolar cancellation of Pr uptake in VCM. A: Same data as in Fig. 4B and C, but Pr uptake by the end of recording (at 300 s) was plotted against the number of pulses. The effect of the matching unipolar pulse at 300 s was taken as 100%. Dashed lines are the best fit logarithmic functions. B: Same as A, but using different x-axes for longer and shorter bipolar nsEP. The axes were shifted against each other so that one 830+830 ns pulse corresponded to 4.15 of 200+200 ns pulses. C: same as A, but plotting Pr uptake against the cumulative duration of all pulses applied. The dashed line is the best logarithmic fit for both 200+200 ns and 830+830 ns pulse data. See Fig. 4 and text for more details. D: A separate set of experiments, where 10, 30 kV/cm pulses (either unipolar 200 ns or bipolar 200+200 ns) were applied at 0.5; 3; or 5 Hz. Pr emission readings at 300 ns were normalized to the effect of unipolar pulse. Mean +/− s.e., n=5-11.

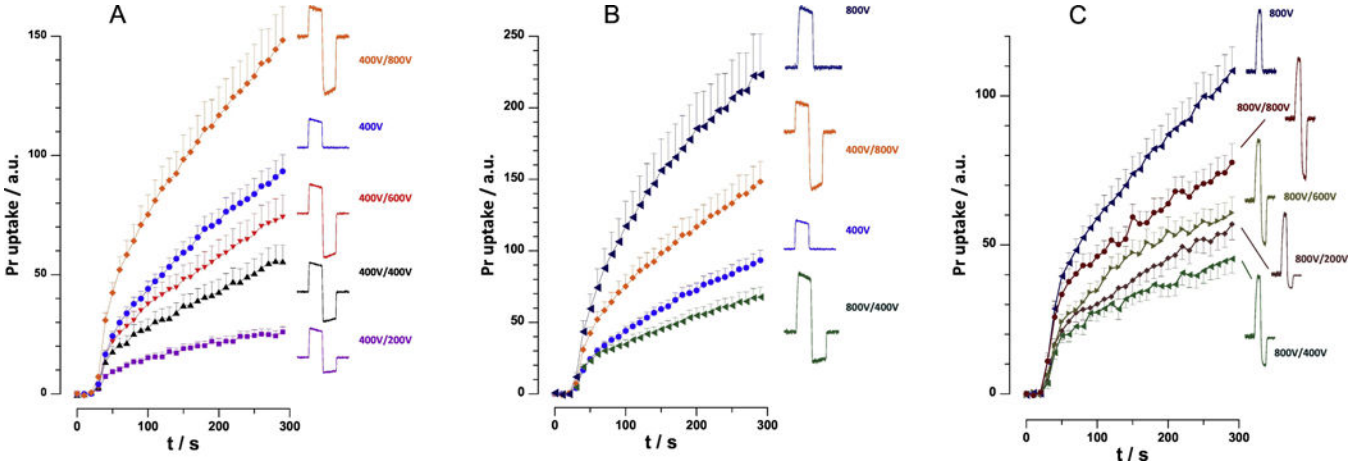

Figure 6.

Effect of the amplitude of the opposite polarity phase of nsEP on electroporation efficiency. Pr uptake was monitored in VCM exposed to trains of 10 uni- or bipolar nsEP, 5Hz, starting at 28 s. The pulse width was 830 ns or 830+830 ns (A and B), and 200 ns or 200+200 ns (C). Pulse amplitude of 800 V translates into 30 kV/cm at the cell location, and smaller amplitudes produce proportionally smaller fields. The configuration of each pulse and the amplitudes of the first/second phases are shown next to the plots. The amplitude of the first phase was kept constant at 400V (A) or at 800V (C) while varying the second phase. In panel B, we specifically compared bipolar pulses with the same spectral content, 400V/800V and 800V/400V, and compared them with respective unipolar pulses; see text for more details. Mean+/− s.e., 15-20 cell per group. Non-overlapping error bars indicate statistically significant difference at $p<0.05$ or better.

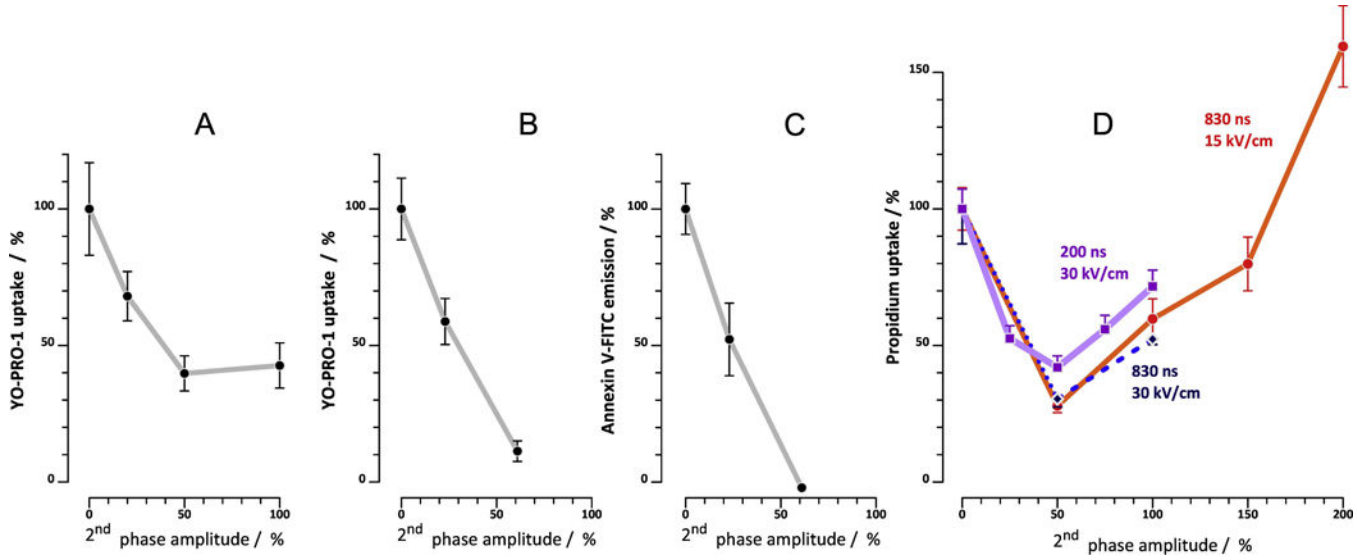

Fig. 7.

Relative amplitude of the 2nd phase determines electroporation efficiency of bipolar nanosecond nsEP. All graphs are plotted from data presented in Figs. 2–6. Maximum effect of bipolar nsEP, as measured by the end of the experiment (300 s for A, B, and D; 200 s for C) is plotted against the amplitude of the 2nd phase of the pulse (the amplitude of the first phase is taken as 100%; "0%" value means unipolar pulse). The magnitude of the effect is expressed in % of the effect of the equivalent unipolar pulse. A: YP uptake in CHO cells after a train of 4 pulses (2 Hz, 9 kV/cm, 230 ns or 230+230 ns, see Fig. 2). B: YP uptake in NEFO-exposed CHO cells (10 pulses, 2 Hz, 7.2 kV/cm; see Fig. 3 and also Fig. 1 for NEFO shape). C: Annexin V-FITC binding in NEFO-exposed U937 cells (50 pulses, 5 Hz, 10 kV/cm; see Fig. 4 and Fig. 1). D: Pr uptake in VCM exposed to a train of 10 nsEP at 5 Hz; other parameters are indicated in the graph. Mean +/− s.e. for 20-50 cells for each datapoint.